International Journal of Thermal Sciences 187 (2023) 108208

Contents lists available at ScienceDirect

International Journal of Thermal Sciences

journal homepage: www.elsevier.com/locate/ijts

Ultrafast thermalization dynamics in Au/Ni film excited by femtosecond laser double-pulse vortex beam

Guangqing Du [a], Fangrui Yu [a], Yu Lu [a], Lin Kai [a], Qing Yang [b], Xun Hou [a], Feng Chen [a,*]

[a] State Key Laboratory for Manufacturing System Engineering and Shaanxi Key Laboratory of Photonics Technology for Information, School of Electronic Science and Engineering, Xi'an Jiaotong University, Xi'an, 710049, PR China
[b] School of Mechanical Engineering, Xi'an Jiaotong University, Xi'an, 710049, PR China

ARTICLE INFO

Keywords:
Thermalization dynamics
Femtosecond laser
Vortex beam
Two-layer film

ABSTRACT

We theoretically investigated ultrafast thermalization dynamics of spatio-temporal evolutions of temperature fields in typical Au/Ni film excited by femtosecond laser double-pulse vortex beam. It is proposed that the enhanced energy deposition in the layered Au/Ni film can be unprecedentedly facilitated via applying femtosecond laser double-pulse vortex beam, preferentially giving rise to vortical thermalization for the phonon system of bottom Ni layer on picosecond timescale. It can be explained as the intensified dynamics of double-pulse vortex beam interacting with the excited intermediate state of Au/Ni film and the following energy competitive processes of the electron thermal diffusion and the electron-phonon coupling in respective layers. Moreover, the electron-phonon coupling period of Au/Ni film with respect to the crucial laser parameters of pulse separation and vortex beam fluence are explored in details. The results can be basically helpful for understanding the ultrafast dynamics of vortical thermalization for advancing the potential applications of compound-cavity fabrication, stimulated emission depletion (STED) imaging and ultrahigh time-resolved spectroscopy, etc.

1. Introduction

Femtosecond laser possessing ultrashort pulse duration and ultrahigh power density has been proved to be an effective tool for exploring advanced applications of materials processing and digging out the novel physics in ultrafast carrier dynamics for new types of materials [1–14]. Physically, as femtosecond laser pulses interact with materials, the two temperature processes are generally considered as the dominant mechanism for regulating ultrafast dynamics of electron and phonon thermalizations in metal targets. It typically falls into time domains ranging from femtosecond-to-picosecond periods which are at least 3 orders of magnitude less than Fourier thermal transfer cycles for target materials [15,16], giving potential merits of reduced thermal diffusion, hence improved processing precision of femtosecond laser interactions with metals.

Recently, it is frequently reported that the femtosecond laser vortex beam can provide even more flexible routes for advanced processing of materials surface than the conventional laser ablation performed with non-vortex pulses [17–22]. The typical optical vortex beam in the form of helical shape has a helical wave front characteristics and annular intensity profile, providing great opportunity for controlling the light-matter interaction processes. Especially, as femtosecond laser vortex beam interacts with functional layered-metal film, the laser pulses depositing routes into the film system can become increasingly diversified in comparation to the single layer film situation. It proposes even higher requirements for flexibly controlling the laser energy deposition into the layered metallic targets for exploring specific light-matter interaction dynamics for advanced applications in fields of compound-cavity fabrication, ultrafast STED imaging and ultrahigh time-resolved spectroscopy, etc. Unfortunately, structuring and modification of layered materials using femtosecond vortex pulses pose a significant challenge due to technical difficulties hindering the synthesis of high-power broadband laser vortex beams and complex energy relaxation across the layered thin film targets. It is reported that double-pulse femtosecond laser can provide the flexible solution for modulating the thermal dynamics in single layer metal film [23–25]. It is highly expected that the ultrafast temperature evolution dynamics in layered-metal film system can also be well manipulated via femtosecond laser double-pulse vortex beam. Nevertheless, the ultrafast thermalization dynamics in layered metallic film system is quite different from the

* Corresponding author.
E-mail address: chenfeng@mail.xjtu.edu.cn (F. Chen).

https://doi.org/10.1016/j.ijthermalsci.2023.108208
Received 31 October 2022; Received in revised form 17 January 2023; Accepted 30 January 2023
Available online 7 February 2023

single layer film heating, which can be especially more complicated in layered film targets as applying femtosecond laser double-pulse vortex beam. Therefore, it needs overall investigations for well understanding of the particular thermal dynamics via shaping the femtosecond laser double-pulse vortex beam. To our best knowledge, the ultrafast thermalization dynamics in two-layer metal film system under particular laser excitations by the femtosecond laser double-pulse vortex beam is not explored so far.

In this paper, we theoretically investigated the ultrafast dynamics of vortical thermalization of electron and phonon systems in typical Au/Ni film by introducing self-consistent thermal dynamics model with respect to the full temperature-dependent thermal and optical properties for the layered film targets. It is revealed that the spatio-temporal evolutions of temperature fields for the electron and phonon systems of Au/Ni film can be well manipulated via applying femtosecond laser double-pulse vortex beam, giving rise to preferential vortical thermalization of phonon system of bottom Ni layer. The intensified dynamics of laser energy deposition governed by the cooperative effect of double-pulse vortex beams coupling into the layered-metal film and the following energy competitive routes in respective film layers are proposed for explanations of the observed vortical thermalization dynamics for electron and phonon systems of the two-layer Au/Ni film.

2. Modeling and methods

The ultrafast thermalization dynamics of femtosecond laser excitation of metallic target obeys the well-known two-temperature model (TTM), in which the thermal equilibrium is broken and rebuilt sequentially from femtoseconds to picoseconds timescales [26,27]. Here, we introduce the self-consistent thermal dynamics model for prediction of two-layer Au/Ni films thermalization under the particular laser excitation of femtosecond double-pulse vortex beam. Physically, as the femtosecond laser double-pulse vortex beam irradiates on the Au/Ni film system, the two-temperature processes can normally occur, in which the electrons in the skin layer of Au/Ni film are initially excited at arrival of the first pulse of double-pulse vortex beam, forming high temperature electron gas in the localized skin layer of Au/Ni film. Then, the high temperature electron gas dissipates its energy to deeper region across the film interface via the electron thermal diffusion channel. Simultaneously, the phonon systems across the interface of two-layer film are locally heated in respective layers due to the localized electron-phonon coupling mechanism. As the second pulse arrives at the surface of Au/Ni film, the pre-excited state of electron system of Au/Ni film will be stimulated again, then goes under way of the two-temperature processes, until the electron and phonon systems get the thermal equilibrium. The two temperature processes typically occur on picoseconds timescale, depending on the particular materials and layered film configurations. The self-consistent thermal dynamics model for description of ultrafast thermal dynamics in two-layer Au/Ni thin films can be mathematically presented as follows:

$$C_e^I \frac{\partial T_e^I}{\partial t} = \nabla\left(k_e^I \nabla T_e^I\right) - g^I\left(T_e^I - T_p^I\right) + S \tag{1}$$

$$C_p^I \frac{\partial T_p^I}{\partial t} = g^I\left(T_e^I - T_p^I\right) \tag{2}$$

$$C_e^{II} \frac{\partial T_e^{II}}{\partial t} = \nabla\left(k_e^{II} \nabla T_e^{II}\right) - g^{II}\left(T_e^{II} - T_p^{II}\right) \tag{3}$$

$$C_p^{II} \frac{\partial T_p^{II}}{\partial t} = g^{II}\left(T_e^{II} - T_p^{II}\right) \tag{4}$$

here, the coupled equation (1) ~ (4) are self-consistently built for well describing the ultrafast thermal excitations and the following multi-route thermal relaxations in Au/Ni film triggered by femtosecond laser double-pulse vortex beam. T_e and T_p denotes the electron and the phonon temperatures, and I, II represents for the surface and bottom layers of Au/Ni film, respectively. C_e and C_p denotes the thermal capacity for electron and phonon systems of Au/Ni film. S accounts for the energy absorption rate of femtosecond laser double-pulse vortex beam with topological charge of $l = \pm 1$, written as

$$S(r,z,t) = \sqrt{\frac{4\ ln\ 2}{\pi}}\ \frac{1-R}{\delta+\delta_b}\sum_{i=1}^{2}\frac{F_i}{t_{pi}}\ \frac{4r^2}{\omega_0^2} exp\Big(/ \omega_0^2\Big) - 2r^2 \times \exp\left[\left(-\frac{z}{\delta+\delta_b}\right) - 4\ ln\ 2\left(\frac{t-2t_{pi}-(i-1)\Delta}{t_{pi}}\right)^2\right] \tag{5}$$

Where r and z is the respective coordinates along the diameter and depth of Au/Ni film. ω_0 is the waist of the corresponding fundamental Gaussian beam, taken as 1.4 μm in simulations. F_i denotes the vortex beam fluence for the ith pulse of femtosecond laser vortex beam. t_{pi} is pulse duration for the ith pulse, which is defined as full width at half maximum. R means the transient surface reflectivity, which is fully considered as the temperature-dependent parameter. δ is the optical skin depth taken as 15.3 nm for surface Au film, and δ_b the electron ballistic transfer length taken as 80 nm here, accounting for the full thickness of Au layer as it is designed to be smaller than 100 nm [28,29]. Δ is the temporal double-pulse separation of femtosecond laser vortex pulses.

As femtosecond laser double-pulse vortex beam excitation of the two-layer Au/Ni film, the dielectric function, which is closely dependent on the transient temperatures of electron and phonon must be taken into account for well exploring the ultrafast thermalization processes in Au/Ni film. The time-dependent complex dielectric function can be split into the real and imaginary parts as follows:

$$\varepsilon = 1 - \frac{\omega_p^2}{\omega^2+\nu_m^2} + i\frac{\nu_m}{\omega}\frac{\omega_p^2}{\omega^2+\nu_m^2} \tag{6}$$

Where $\omega_p^2 = \frac{e^2 n_e}{\varepsilon_0 m_e}$, denotes the plasma frequency of metallic film materials. Here, n_e and m_e represents the electron density and mass , respectively. The total scattering rate of electrons can be written in the form of the sum of rates of the separate mechanisms: $\nu_m = 1/\tau_{ee} + 1/\tau_{ep}$, where τ_{ee} and τ_{ep} are the electron-electron and electron-phonon scattering time, depending on electron and phonon temperatures, written as $\tau_{ee} = 1/A_e T_e^2$ and $\tau_{ep} = 1/B_p T_p^2$, respectively. Applying the Fresnel law at the Au film surface, we get the temperature-dependent reflectivity coefficient as follows:

$$R = \frac{\left[Re\left(\sqrt{\varepsilon}\right)-1\right]^2 + \left[Im\left(\sqrt{\varepsilon}\right)\right]^2}{\left[Re\left(\sqrt{\varepsilon}\right)+1\right]^2 + \left[Im\left(\sqrt{\varepsilon}\right)\right]^2} \tag{7}$$

In this model, the temperature-dependent thermal parameters are fully taken into account for investigations of the thermal dynamics in two-layer Au/Ni film with respect to the collaborative mechanism of laser energy coupling into targets following double-pulse vortex beam excitations. The commonly used approximation for electron thermal capacity of $C_e = \gamma T_e$ is adopted here and the electron thermal conductivity k_e is considered as a wide range of electron temperature dependent parameter during the electron-phonon coupling period, written as [30]:

$$k_e = \chi\frac{\left(\theta_e^2+0.16\right)^{5/4}\left(\theta_e^2+0.44\right)\theta_e}{\left(\theta_e^2+0.092\right)^{1/2}\left(\theta_e^2+\eta\theta_p\right)} \tag{8}$$

Here, $\theta_e = T_e/T_F$, $\theta_p = T_p/T_F$, $\eta = 0.16$, $\chi = 353 \mathrm{Wm^{-1}K^{-1}}$ for surface Au film. The temperature-dependent electron–phonon coupling strength was proposed by Zhang and Chen, which can be analytically represented as follows [30]:

$$g = g_0\left[A_e \,/\, B_p\left(T_e + T_p\right) + 1\right] \tag{9}$$

where, g_0 is the electron–phonon coupling strength in room temperature, and the coefficients A_e and B_p are constants, depending on the material properties of different film layers.

Because of the flexibility of Finite Element Method (FEM) in dealing with coupled transient heat transfer equations, the coupling partial differential Eq. (1)~(4) are simultaneously solved by applying the commercial software package of COMSOL Multiphysics. In this simulation, it is reasonable to assume that the heat energy loss from the Au/Ni film system to the front surface can be neglected during femtosecond-to-picosecond periods, and the perfect thermal insulation is assumed at rear surface and bilateral sides of the two-layer film system. For the interior interface of the two-layer film system, the electron system exhibits perfect thermal conductivity due to high electron collision rate across the film interface, facilitating perfect electron thermal coupling on femtosecond-to-picosecond timescales. However, the phonon system normally exhibits thermal jump at the film interface because of quite large phonon mass compared to electron system, leading to very large phonon thermal resistance across the interface of Au/Ni film during femtosecond-to-picosecond periods.

3. Results and discussions

In this simulation, the femtosecond laser source is treated as non-focused vortex beam. Before it reaches the surface of Au/Ni film, the distribution of laser fluence of vortex beam with topological charge of $l = \pm 1$ can be considered as a function of radius coordinate r and time t, written as:

$$F(r,t) = eF_p\left(\frac{2r^2}{\omega_0^2}\right)\exp\left(-\frac{2r^2}{\omega_0^2}\right)\exp\left[4\,ln\,2\left(\frac{t - t_{pi} - (i-1)\Delta}{t_{pi}}\right)^2\right] \tag{10}$$

Where F_p is the maximal fluence value corresponding to the bright edge of the vortex beam. At a given time of temporal peak of the pulse, the normalized spatial profile of vortex beam spot in air is mapped in Fig. 1 (a), the extracted line profile is plotted in Fig. 1 (b). It can be clearly seen that the vortex beam spot exhibits a zero fluence at the beam center ($r/r_p = 0$) and two symmetric peaks of bright edge at the positions ($r/r_p = \pm 1$), where r_p is written as $r_p = \omega_0/\sqrt{2}$. Generally, the spatial fluence profile of vortex beam spot can remain its shape unchanged before it reaches the surface of Au/Ni film due to ignorable absorption of vortex beam propagation in air. Nevertheless, the laser absorption in Au/Ni film definitely plays a crucial role in the ultrafast thermalization dynamics of the layered film system, which will be investigated in details in the following sections.

The 2-D images of spatio-temporal evolutions of the electron and phonon temperature fields in two-layer Au/Ni film excited by femtosecond laser double-pulse vortex beam is shown in Fig. 2. It should be emphasized that the current 2D modeling can be qualified for description of the vortex beam excitations of full 3D Au/Ni film due to rotational symmetry of the two-layer film geometry and the vortex beam for saving computation load. The relevant simulation parameters for Au and Ni are used as follows [31,32]: For Au film, $g_0 = 0.21 \times 10^{17}$ $Jm^{-3}s^{-1}K^{-1}$, $\gamma = 68$ $Jm^{-3}K^{-2}$, $C_p = 2.5 \times 10^6 Jm^{-3}K^{-1}$, $A_e = 1.18 \times 10^7 s^{-1}K^{-2}$, $B_p = 1.25 \times 10^{11}$ $s^{-1}K^{-1}$. For Ni film, $g_0 = 3.6 \times 10^{17}$ $Jm^{-3}s^{-1}K^{-1}$, $\gamma = 1065$ $Jm^{-3}K^{-2}$, $C_p = 4.1 \times 10^6$ $Jm^{-3}K^{-1}$, $A_e = 0.14 \times 10^7$ $s^{-1}K^{-2}$, $B_p = 1.4 \times 10^{11}$ $s^{-1}K^{-1}$. It can been seen that the electron system is dominantly heated in skin layer of surface Au layer [Fig. 2 (a)]. Also, it clearly exhibits the annular-shaped temperature profile of surface vortical thermalization for electron system, in which the obvious two-edged high temperature zones and the central low temperature point correspond to the two of maxima bright edges and dark center of the femtosecond laser vortex beam.

We can see that with time at 1 ps, the annular-shaped vortical temperature field of electron system in surface Au film layer exhibits evident drop, simultaneously penetrating into inner interface region of Au/Ni films [Fig. 2(b)]. As the second femtosecond pulse subsequently arrives at surface of Au/Ni film at 2.088 ps, the electron system is violently stimulated again, leading to raised vortical temperature of electron system, which is evaluated to a value as high as 6647 K at maxima of bright edge of the femtosecond laser vortex beam [Fig. 2(c)]. Nevertheless, the electron temperature field is successively declined until time at 14 ps, accounting for the termination of electron-phonon coupling processes [Fig. 2(d)]. In another hand, the phonon system across Au/Ni film almost keeps undisturbed at 88 fs as seen from Fig. 2(e). However, the vortical thermalization of phonon system are initially engaged for Au and Ni films at 1 ps, producing observable annular-shaped temperature fields in the surface layer of Au/Ni film [Fig. 2(f)]. In fact, the electron-phonon coupling mechanism takes place in ballistic electron excitation region in effective skin layer, which covers the full Au film thickness of 80 nm, leading to the observed results of elevated vortical thermalization in Au layer of Au/Ni film at 1 ps. With time, the phonon temperature field exhibits layering vortical thermalization across the interface of Au/Ni film at 2.088 ps, in which the vortical phonon system for bottom Ni layer is preferentially heated compared to surface Au film [Fig. 2(g)]. It can be attributed to the competitive energy transfer processes of the electron thermal diffusion and the electron-phonon coupling in respective layers of Au/Ni film, in which the dominant phonon heating governed by the electron-phonon coupling mechanism in Ni layer is definitely intensified due to the larger electron-phonon coupling strength for Ni film compared to Au film. Here, the phonon thermal diffusions between the Au and Ni film layers are reasonably ignored due to the ultrafast thermal dynamics processes safely falling into the femtosecond-to-picosecond regime, which are at least 3 orders of magnitude less than Fourier phonon thermal diffusion cycles.

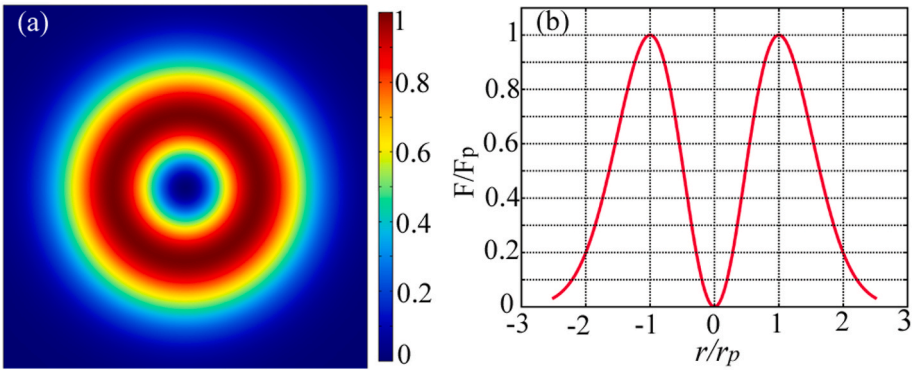

Fig. 1. The normalized spatial profile of vortex beam spot before it reaches the surface of Au/Ni film. (a) The 2D distribution of laser fluence of vortex beam spot. (b) The extracted line profile of laser fluence of vortex beam spot.

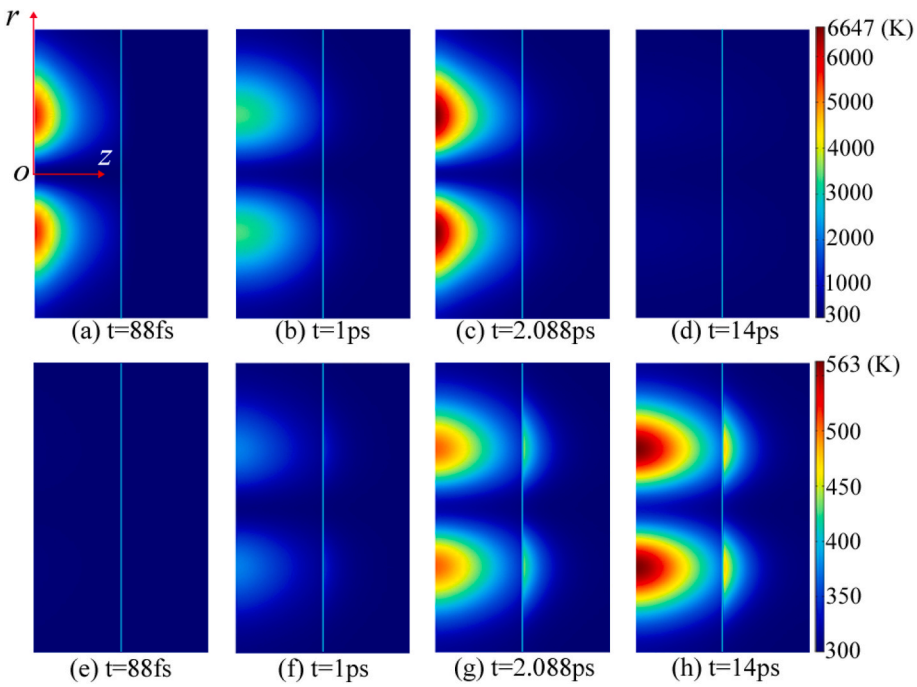

Fig. 2. The 2-D images of spatio-temporal evolutions of electron and phonon temperature fields in two-layer Au/Ni film excited by femtosecond laser double-pulse vortex beam. The pulse separation of double-pulse vortex beam is 2 ps, the respective pulse fluence is set as 0.2 J/cm^2. The pulse duration 30fs for respective pulses of double-pulse vortex beam. Electron temperature at different evolutions time: (a) 88 fs, (b)1 ps, (c) 2.088 ps, (d) 14 ps; Phonon temperature at different evolutions time: (e) 88 fs, (f)1 ps, (g) 2.088 ps, (h) 14 ps.

Ultimately, the layering vortical thermalization processes across the interface are further intensified until 14 ps [Fig. 2(h)], namely a time for the electron and phonon system getting their unified vortical temperature in Au/Ni film. After that, the Fourier phonon thermal diffusion will dominate the thermal relaxation processes, not shown here, which are not the scope of currently focused investigations for the ultrafast nonequilibrium vortical thermalization dynamics in Au/Ni film.

The surface vortical temperature fields for the electron and phonon systems of Au/Ni film excited by femtosecond laser double-pulse vortex beam for different total fluences are shown in Fig. 3. Here, the surface vortical temperature field for the electron system is defined at the maximal peak of electron temperature envelope. It indicates the extremely nonequilibrium intermediate state in Au/Ni film, which typically occurs after arrival of the second pulse of femtosecond laser double-pulse vortex beam. Nevertheless, the vortical phonon temperature is defined as available maximal one, normally appearing at time of the electron-phonon coupling termination at 14 ps. We can see from Fig. 3(a) that the surface vortical temperature fields for electron system are obviously elevated at the symmetrical bright edges compared to the dark center of vortex beam at fluences of 0.1 J/cm^2, 0.2 J/cm^2 and 0.3 J/cm^2, respectively. It can be seen from Fig. 3(b) that the vortical phonon temperature field on surface of Au/Ni film has the similar profile to the electron temperature field, which is typically originated from the electron-phonon coupling mechanism and ignored phonon thermal diffusion for locally transferring the absorbed laser energy from electron system to phonon system during the electron-phonon coupling period. More interestingly, we can see in Fig. 3(b) that the surface vortical phonon temperature at the dark center of vortex beam is observably evalated for a larger fluence of 0.3 J/cm^2 compared to 0.2 J/cm^2 and 0.1 J/cm^2. It can be well explained as the transversal electron thermal diffusion along the surface dimension and the localized electron-phonon coupling in the Au/Ni film at neighbouring of the dark center of vortex beam, which can be significantly boosted via applying higher laser fluence of femtosecond double-pulse vortex beam. The results can be provide basic guideline for managing the vortical fields of surface electron and phonon temperature for Au/Ni film thermalization via optimizing the laser fluence of vortex beam, potentially benefiting for a wide range of applications like annular heating, ultrafast STED imaging and ultrahigh time-resolved spectroscopy, etc.

The ultrafast dynamics of double-pulse vortex beam interacting with the excited intermediate state of Au/Ni film for regulating the transient surface reflectivity of femtosecond laser double-pulse vortex beam can play a unique role in affecting the totally laser pulses energy coupling into the two-layer Au/Ni film. In the current model, we take the temperature-dependent dielectric function for the surface Au film. The surface reflectivity is calculated according to the well-known Fresnel formula, which is fully taken as temperature-dependent function. Therefore, the temperature-dependent dielectric function definitely

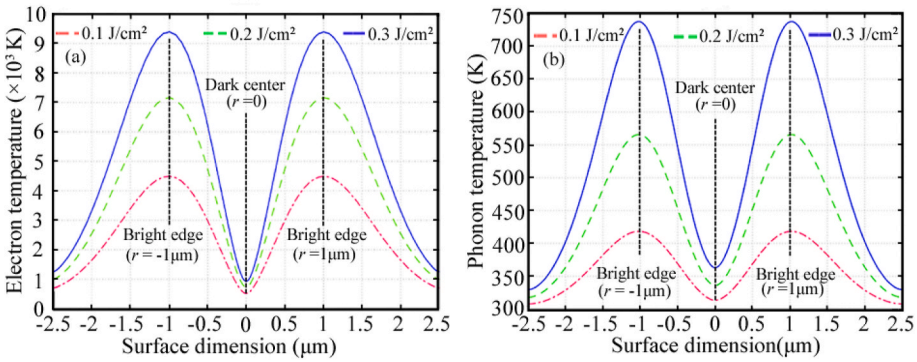

Fig. 3. The surface vortical temperature fields for the electron and phonon systems of Au/Ni film excited by femtosecond laser double-pulse vortex beam for different total fluences. The pulse separation is 1 ps, the laser lavelength 800 nm, pulse duration 30 fs, and the vortex topological charge of $l = \pm 1$ are set for the respective pulses of femtosecond laser double-pulse vortex beam. (a) The surface vortical temperature fields for electron system(a); (b) The surface vortical temperature fields for phonon system.

gives rise to modifications of the transient reflectivity, which can be especially modified via tuning the pulse separation of double femtosecond pulses. Fig. 4 shows the transient surface reflectivity on Au/Ni film at peak of the second pulse via modifying the pulse separation of femtosecond laser double-pulse vortex beam. The transient surface reflectivity at peak of the first pulse are plotted for comparation purpose. It can be seen from Fig. 4(a) that at the double-pulse separation of 500 fs, compared to the first pulse, the surface transient reflectivity of the second pulse is declined, which gets as low as 0.741 at the maxima of bright edges of vortex beam. With double-pulse separation at 1 ps, the transient reflectivity for first pulse keeps unchanged, but the transient reflectivity of the second pulse slightly rises to 0.752 [Fig. 4(b)]. We can see that as double-pulse separation increases to 4 ps, the surface transient reflectivity for the second pulse becomes slightly differentiating in contrast to first pulse [Fig. 4(c)]. The surface transient reflectivity for the first and second femtosecond pulses exhibits even less difference at pulse separation of 7 ps [Fig. 4(d)]. In fact, as continuously increasing the double-pulse separation, the difference of surface transient reflectivity for the respective pulses of femtosecond laser double-pulse vortex beam gets saturation until the pulse separation gets the electron-phonon coupling period of 14 ps, which is not shown here.

The results can be well explained as the intensified dynamics of cooperative double-pulse vortex beam coupling with the excited intermediate state of Au/Ni film, which - closely relates to the pulse separation of femtosecond laser double-pulse vortex beam. As for a smaller pulse separation, the first leading pulse can be largely beneficial for excitation of sub-surface and hance preheating of effective skin layer of Au/Ni film, leading to high-temperature driven scattering state of electron system for enhancing the second pulse coupling into the target. With increasing the double-pulse separation, the electron temperature for the preheated intermediate state can be lowered due to the sustaining electron-phonon coupling process for dissipating the temperature of high-temperature electrons to local phonon on picosecond timescale. As a result, as increasing double-pulse separation in picosecond time domain, the surface transient reflectivity discrepancy becomes smaller for the respective pulses of femtosecond laser double-pulse vortex beam. Once the pulse separation gets close to a time comparable to the electron-phonon coupling period calculated as 14ps in this simulation, the second pulse will totally interact with recovered excitation state at termination of the electron-phonon coupling period, leading to invalidity of the merit of enhanced coupling of laser energy into the layered target by using the femtosecond laser double-pulse vortex beam.

The spatio-temporal distributions of electron and phonon temperature fields for Au/Ni film at bright edge and dark center of femtosecond laser double-pulse vortex beam are shown in Fig. 5. We can see from Fig. 5(a) that the temporal profile of surface electron temperature field exhibits sharp two-peaks trait at the brightest edge in comparation to dark center of the femtosecond laser vortex beam. Also, the temporal profile of temperature field for the electron system can be severely weakened at the interface of Au/Ni film compared to film surface due to the increased degeneration of the electron thermal diffusion in depth direction, simultaneously blurring sharp temporal profile of the electron temperature at interface region [Fig. 5(b)]. We can see that the temporal profile of surface phonon temperature field correspondingly exhibits two-step heating processes at the brightest edge in comparation to dark center of the femtosecond laser vortex beam as seen in Fig. 5(c). Compared to the dark center of femtosecond laser double-pulse vortex beam, the maximal surface phonon temperature at brightest edge of the vortex beam gets 560 K at termination of the electron-phonon coupling period at 14 ps. It can be seen from Fig. 5 (d) that the surface electron temperature is obviously cut down and two-peaks profile becomes significantly blunt at the interface region compared to brightest edge on Au/Ni film surface. The electron and phonon temperatures at bright edge and dark center of vortex beam along the depth of Au/Ni film at termination of electron-phonon coupling period is shown in Fig. 5(e) and (f). We can see from Fig. 5(e) that the electron temperature fields have smooth transition across the interface of Au/Ni film at both the dark center and brightest edge of vortex beam. However, the preferentially layering vortical thermalization at interface of Au/Ni film can be

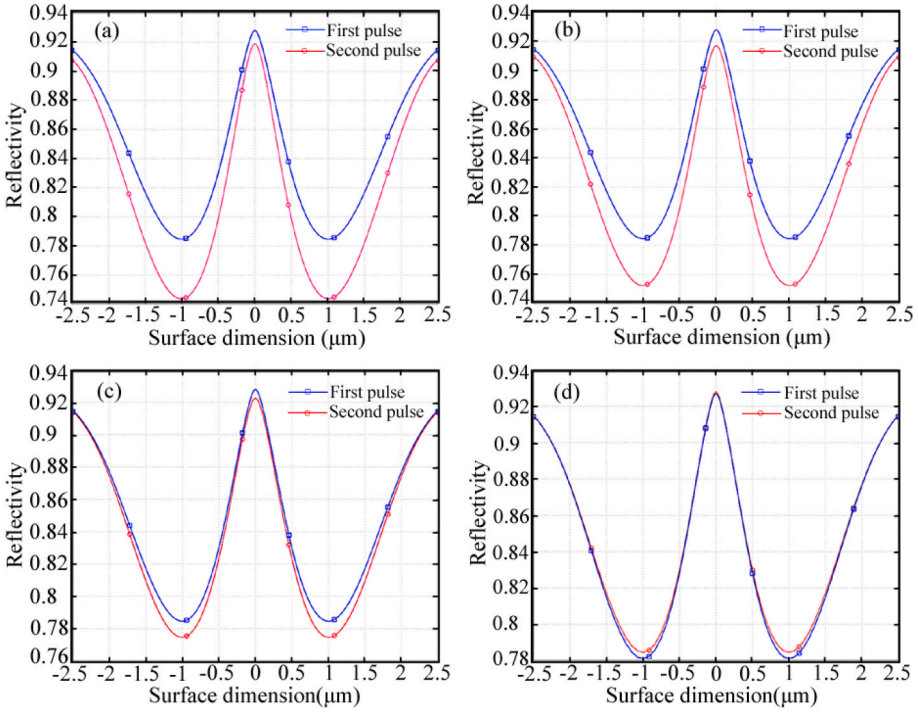

Fig. 4. The transient reflectivity on surface of Au/Ni two layer film with respect to laser excitations of femtosecond laser double-pulse vortex beam. The respective pulse fluence is set as $F_1 = F_2 = 0.2$ J/cm^2. The pulse duration is 30fs for respective pulses of double-pulse vortex beam. The pulse separation of double-pulse vortex beam is (a) 500 fs, (b) 1 ps, (c) 4 ps, and (d) 7 ps, respectively.

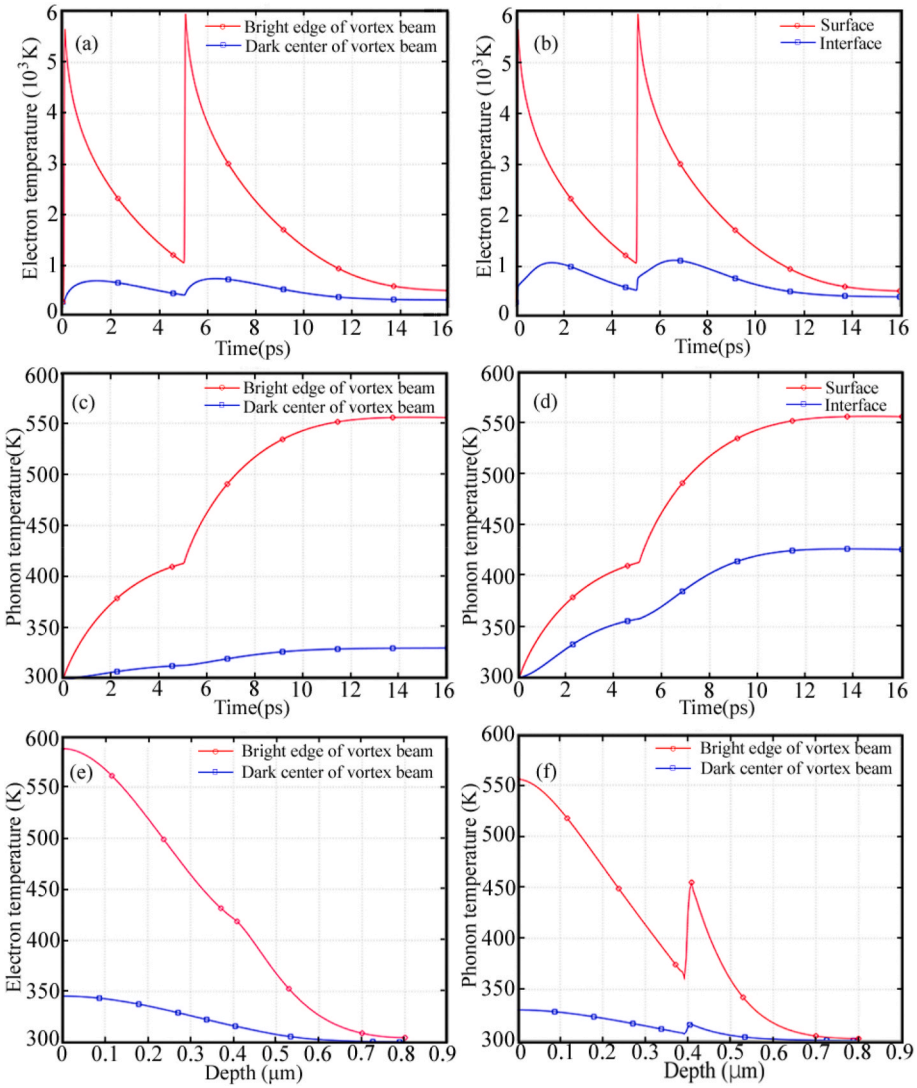

Fig. 5. The spatio-temporal fields of electron and phonon temperatures for the Au/Ni film excited by femtosecond laser double-pulse vortex beam. The pulse separation is 5 ps, the fluence of respective pulse is set as 0.2 J/cm^2. The laser wavelength 800 nm, pulse duration 30fs and the vortex topological charge of $l = \pm 1$ are taken for the respective pulses of the femtosecond laser double-pulse vortex beam. (a) Electron temperatures at bright edge and dark center of vortex beam; (b) Electron temperatures at surface and interface of Au/Ni film; (c) Phonon temperature at bright edge and dark center of vortex beam; (d) Phonon temperatures at surface and interface of Au/Ni film; (e) Depth distributions of electron temperatures; (f) Depth distributions of phonon temperatures.

evidently observed for phonon system along the depth Au/Ni film, especially from the surface point at the brightest edge of the vortex beam after termination of the electron-phonon coupling period as seen in Fig. 5(f). The difference of the electron and phonon temperature fields at the interface can be mainly attributed to the dislike thermal conductivity behaviours for the electron and phonon systems on picosecond timescale, in which the electron thermal conductivity is considered as continuous across the interface, but the phonon thermal conductivity is reasonably taken as incontinuous one due to the significant larger thermal capacity of phonons compared to electrons system. The preferential vortical thermalization of phonon system of bottom Ni film can be engaged based on the fact that the electron-phonon coupling strength

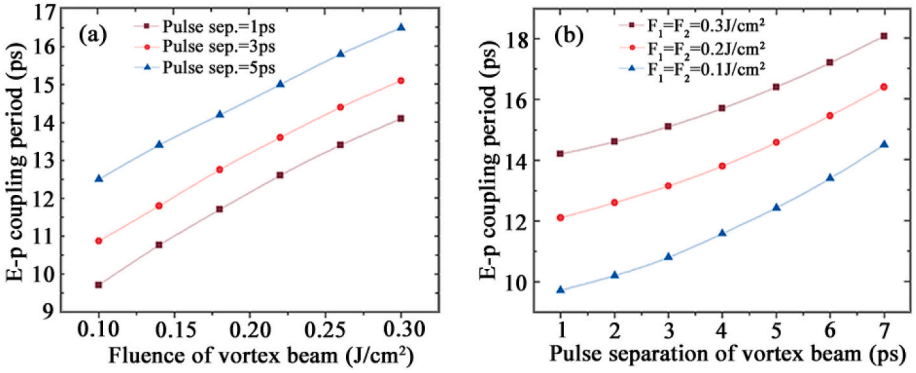

Fig. 6. The electron-phonon coupling period with respect to total laser fluence and pulse separation of femtosecond laser double-pulse vortex beam. The laser wavelength 800 nm, pulse duration 30fs and the vortex topological charge of $l = \pm 1$ are employed for the respective pulses of the femtosecond laser double-pulse vortex beam. (a) Total laser fluence modifications; (b) Pulse separation variations.

for bottom Ni film (3.6×10^{17} Jm^{-3} $s^{-1}K^{-1}$) is an order of magnitude larger compared suface Au film (0.21×10^{17} Jm^{-3} $s^{-1}K^{-1}$).

The electron-phonon coupling dynamics plays a crucial role in governing the phonon vortical thermalization in two-layer Au/Ni film system. Fig. 6 shows the electron-phonon coupling period for Au/Ni film excited by femtosecond laser double-pulse vortex beam. Here, the identical configurations of pulse duration, wavelength and vortex topological charge are taken for respective pulses of femtosecond laser double-pulse vortex beam, but having adjustable pulse separation and total pulse fluence of them. The laser lavelength centered at 800 nm, pulse duration 30fs and the vortex topological charge of ±1 are employed for the simulations. We can see from Fig. 6(a) that the electron-phonon periods of Au/Ni film exhibits near-linear extention with increasing the total fluence for different double-pulse separations of 1 ps, 3ps and 5 ps, respectively. It can be seen from Fig. 6(b) that the electron-phonon coupling period for Au/Ni film can be obviously prolonged with near-linear trendency as increasing the pulse separation of femtosecond laser double-pulse vortex beam. It shows that the crucial parameters of laser fluence and double-pulse separation can be definitely qualified for linearly manipulating the electron-phonon coupling process, giving rise to possibly controlling the vortical thermalization of phonon system for Au/Ni two layer film. However, it should be emphasized that employing very large laser fluence of the femtosecond laser double-pulse vortex beam can definitely support for fast phonon thermalization process, adversely giving rise to possible degradation of phonon excitation accuracy due to the early thermal diffusion cycle for phonon system possibly overlaps with the significantly prolonged electron-phonon coupling period of the layered metal film target. The results can be basically important for understanding the ultrafast thermalization of layered metal films excited by femtosecond laser double-pulse vortex beam, qualified for a wide range of applications of laser excitation and processing of layered film, such as compound cavity fabrication, ultrafast STED imaging and time-resolved spectroscopy, etc.

4. Conclusion

We theoretically investigated the ultrafast dynamics of spatio-temporal temperature evolutions for Au/Ni two-layer film excited by femtosecond laser double-pulse vortex beam. It is found that the layering vortical thermalization are observably emerged across the interface of Au/Ni film during the electron-phonon coupling period, in which the vortical phonon system for bottom Ni layer is preferentially heated compared to surface Au film. It can be attributed to the enhanced laser energy coupling across the interface of Au/Ni film as a result of the successive electron thermal diffusion and dominant vortical heating for phonon system in Ni film due to larger electron-phonon coupling strength for Ni film compared to Au film. In addition, it is revealed that the electron-phonon coupling period can be near-linearly prolonged by increasing separation or laser fluence of femtosecond laser double-pulse vortex beam. The results can be basically helpful for well understanding the controllable thermalization dynamics in layered metal film via femtosecond laser double-pulse vortex beam excitations for advancing a wide range of applications of laser micro-annular cavity fabrication, ultrafast STED imaging and ultrahigh time-resolved spectroscopy, etc.

Declaration of competing interest

The authors declare that they have no known competing financial interests or personal relationships that could have appeared to influence the work reported in this paper.

Data availability

Data will be made available on request.

Acknowledgements

This work is supported by the National Science Foundation of China under the Grant nos. 12127806, 62175195, 61875158, the International Joint Research Laboratory for Micro/Nano Manufacturing and Measurement Technologies, the Fundamental Research Funds for the Central Universities.

References

[1] H.W. Liu, F. Chen, X.H. Wang, Q. Yang, D.S. Zhang, J.H. Si, X. Hou, Photoetching of spherical microlenses on glasses using a femtosecond laser, Opt Commun. 282 (2009) 4119–4123.
[2] F. Chen, Z.F. Deng, Q. Yang, H. Bian, G.Q. Du, J.H. Si, X. Hou, Rapid fabrication of a large-area close-packed quasi-periodic microlens array on BK7 glass, Opt. Lett. 39 (2014) 606–609.
[3] J.L. Yong, Q. Yang, X. Hou, F. Chen, Nature-inspired superwettability achieved by femtosecond lasers, Ultrafast Science 2022 (2022) 1–51.
[4] J.L. Yong, Q. Yang, F. Chen, D.S. Zhang, G.Q. Du, H. Bian, J.H. Si, X. Hou, Bioinspired superhydrophobic surfaces with directional adhesion, RSC Adv. 4 (2014) 8138–8143.
[5] J.L. Yong, C.J. Zhang, X. Bai, J.Z. Zhang, Q. Yang, X. Hou, F. Chen, Designing "Supermetalphobic" surfaces that greatly repel liquid metal by femtosecond laser processing: does the surface chemistry or microstructure play a crucial role? Adv. Mater. Interfaces. 7 (2020), 190193.
[6] S.G. He, F. Chen, K.Y. Liu, Q. Yang, H.W. Liu, H. Bian, X.W. Meng, C. Shan, J.H. Si, Y.L. Zhao, X. Hou, Fabrication of three-dimensional helical microchannels with arbitrary length and uniform diameter inside fused silica, Opt. Lett. 37 (2012) 3825–3827.
[7] J.L. Yong, F. Chen, J.L. Huo, Y. Fang, Q. Yang, B. Hao, W.T. Li, Y. Wei, Y.Z. Dai, X. Hou, Green, biodegradable, underwater superoleophobic wood sheet for efficient oil/water separation, ACS Omega 3 (2018) 1395–1402.
[8] J.L. Yong, S.C. Singh, Z.B. Zhan, F. Chen, C.L. Guo, How to obtain six different superwettabilities on a same microstructured pattern: relationship between various superwettabilities in different solid/liquid/gas systems, Langmuir 35 (2019) 921–927.
[9] Q.M. Zhang, H. Lin, B.H. Jia, L. Xu, M. Gu, Nanogratings and nanoholes fabricated by direct femtosecond laser writing in chalcogenide glasses, Opt Express 18 (2010) 6885–6890.
[10] A.D. Wang, L. Jiang, X.W. Li, Y. Liu, X.Z. Dong, L.T. Qu, X.M. Duan, Y.F. Lu, Mask-free patterning of high-conductivity metal nanowires in open air by spatially modulated femtosecond laser pulses, Adv. Mater. 27 (2015) 6238–6243.
[11] R. Buividas, S. RekŠtytė, M. Malinauskas, S. Juodkazis, Nano-groove and 3D fabrication by controlled avalanche using femtosecond laser pulses, Opt. Mater. Express 3 (2013) 1674–1686.
[12] Q.M. Bian, X.M. Yu, B.Z. Zhao, Z.H. Chang, S.T. Lei, Femtosecond laser ablation of indium tin-oxide narrow grooves for thin film solar cells, Opt Laser. Technol. 45 (2013) 395–401.
[13] C. Zheng, A.M. Hu, K.D. Kihm, Q. Ma, R.Z. Li, T. Chen, W.W. Duley, Femtosecond laser fabrication of cavity microball lens (CMBL) inside a PMMA substrate for super-wide angle imaging, Small 11 (2015) 3007–3016.
[14] J. Keloth, K.P. Nayak, K. Hakuta, Fabrication of a centimeter-long cavity on a nanofiber for cavity quantum electrodynamics, Opt. Lett. 42 (2017) 1003–1006.
[15] L.L. Taylor, R.E. Scott, J. Qiao, Integrating two-temperature and classical heat accumulation models to predict femtosecond laser processing of silicon, Opt. Mater. Express 8 (2018) 648–658.
[16] S.L. Sobolev, Nonlocal two-temperature model: application to heat transport in metals irradiated by ultrashort laser pulses, Int. J. Heat Mass Tran. 94 (2016) 138–144.
[17] J.J.J. Nivas, E. Allahyari, F. Cardano, A. Rubano, R. Fittipaldi, A. Vecchione, D. Paparo, L. Marrucci, R. Bruzzese, S. Amoruso, Vector vortex beams generated by q-plates as a versatile route to direct fs laser surface structuring, Appl. Surf. Sci. 471 (2019) 1028–1033.
[18] L. Yang, D.D. Qian, C. Xin, Z.J. Hu, S.Y. Ji, D. Wu, Y.L. Hu, J.W. Li, W.H. Huang, J. R. Chu, Direct laser writing of complex microtubes using femtosecond vortex beams, Appl. Phys. Lett. 110 (2017) 1–5.
[19] H.C. Cheng, P. Li, S. Liu, P. Chen, L. Han, Y. Zhang, W. Hu, J.L. Zhao, Vortex-controlled morphology conversion of microstructures on silicon induced by femtosecond vector vortex beams, Appl. Phys. Lett. 111 (2017) 1–5.
[20] J.J.J. Nivas, S.T. He, A. Rubano, A. Vecchione, D. Paparo, L. Marrucci, R. Bruzzese, S. Amoruso, Direct femtosecond laser surface structuring with optical vortex beams generated by a q-plate, Sci. Rep. 5 (2015) 1–12.
[21] Y. Tang, W. Perrie, D.R. Sierra, Q.L. Li, D. Liu, S.P. Edwardson, G. Dearden, Laser-material interactions of high-quality ultrashort pulsed vector vortex beams, Micromachines 12 (2021) 1–15.
[22] M.G. Rahimian, A. Jain, H. Larocque, P.B. Corkum, E. Karimi, V.R. Bhardwaj, Spatially controlled nano-structuring of silicon with femtosecond vortex pulses, Sci. Rep. 10 (2020), 12643.
[23] S. Gao, X.W. Li, Y.L. Lian, S.P. Zhou, X.Y. Zhang, Z.Y. Fu, J. Huang, Alternate morphology evolution of bulge structures on thin gold films induced by internal stress distribution adjusted by femtosecond laser double-pulse, Opt Laser. Technol. 151 (2022) 1–8.

[24] F. Fraggelakis, G. Mincuzzi, J. Lopez, I. Manek-Hönninger, R. Kling, Controlling 2D laser nano structuring over large area with double femtosecond pulses, Appl. Surf. Sci. 470 (2019) 677–686.
[25] K. Takenaka, N. Shinohara, M. Hashida, M. Kusaba, H. Sakagami, Y. Sato, S. Masuno, T. Nagashima, M. Tsukamoto, Delay times for ablation rate suppression by femtosecond laser irradiation with a two-color double-pulse beam, Appl. Phys. Lett. 119 (2021) 1–6.
[26] S.I. Anisimov, B.L. Kapeliovich, T.L. Perelman, Electron emission from metal surfaces exposed to ultrashort laser pulses, Sov. Phys. JETP 39 (1974) 375–377.
[27] V. Schmidt, W. Husinsky, G. Betz, Ultrashort laser ablation of metals: pump–probe experiments, the role of ballistic electrons and the two-temperature model, Appl. Surf. Sci. 197 (2002) 145–155.
[28] J.K. Chen, J. E Beraun, L.E. Grimes, D.Y. Tzou, Modeling of femtosecond laser-induced non-equilibrium deformation in metal films, Int. J. Solid Struct. 39 (2022) 3199–3216.
[29] J. Hohlfeld, J.G. Müller, S.-S. Wellershoff, E. Matthias, Time-resolved thermoreflectivity of thin gold films and its dependence on film thickness, Appl. Phys. B 64 (1997) 387–390.
[30] J.K. Chen, D.Y. Tzou, J.E. Beraun, A semiclassical two-temperature model for ultrafast laser heating, Int. J. Heat Mass Tran. 49 (2006) 307–316.
[31] Z.B. Lin, L.V. Zhigilei, Temperature dependences of the electron–phonon coupling, electron heat capacity and thermal conductivity in Ni under femtosecond laser irradiation, Appl. Surf. Sci. 253 (2007) 6295–6300.
[32] A.M. Chen, H.F. Xu, Y.F. Jiang, L.Z. Sui, D.J. Ding, H. Liu, M.X. Jin, Modeling of femtosecond laser damage threshold on the two-layer metal films, Appl. Surf. Sci. 257 (2010) 1678–1683.